Surface Roughness in Metal Material Extrusion 3D Printing: The Influence of Printing Orientation and the Development of a Predictive Model

Cuong Nguyen Van
Faculty of Mechanical Engineering, University of Transport and Communications, Vietnam
nguyencuong@utc.edu.vn

Anh Le Hoang
Faculty of Mechanical Engineering, Vinh Long University of Technology Education, Vietnam
anhlh@vlute.edu.vn (corresponding author)

Cao Dang Long
Faculty of Mechanical Engineering, Vinh Long University of Technology Education, Vietnam
caodanglong.quatest3@gmail.com

Duy Nguyen Hoang
Faculty of Mechanical Engineering, Vinh Long University of Technology Education, Vietnam
duynh@vlute.edu.vn

Received: 4 July 2023 | Revised: 22 July 2023 | Accepted: 24 July 2023

 DOI: https://doi.org/10.48084/etasr.6162

ABSTRACT

This study investigates the influence of printing orientation on the surface roughness in metal material extrusion 3D printing of 17-4 PH stainless steel. Experimental tests were conducted on the Markforged Metal X commercial 3D printer at Vinh Long University of Technology Education, Vietnam. The samples were printed in three different orientations: flat, on-edge, and upright. Surface roughness measurements were performed using a handheld Mitutoyo SJ-210 roughness tester. Quantitative analysis of the surface roughness measurements revealed significant variations among the different printing orientations. The upright orientation exhibited the smoothest surface, with an average R_a value of 7.42 µm and R_z value of 40.49 µm. In contrast, the flat orientation showed the highest roughness, with an average R_a value of 82.83 µm and R_z value of 109.32 µm. The on-edge orientation had intermediate roughness values, with an average R_a value of 69.42 µm and R_z value of 92.17 µm. The study also introduces a novel predictive model for surface roughness based on the printing parameters. The model demonstrated accurate estimations for surface roughness values in specific cases, enabling optimization of the printing process for desired surface quality.

Keywords-additive manufacturing; material extrusion; 17-4 PH stainless steel; building orientation; microstructure; mechanical properties

I. INTRODUCTION

Additive Manufacturing (AM) or 3D printing is a production process that allows the creation of products by adding material layer by layer to form detailed components from a 3D digital model [1-4]. The ASTM/ISO standards classify metal 3D printing technologies into 7 different groups: Material Extrusion (ME), Material Jetting (MJ), Binder Jetting (BJ), VAT photopolymerization, Powder Bed Fusion (PBF), Direct Energy Deposition (DED), and sheet object lamination (ASTM ISO/ASTM52900-15, 2015). ME technology accounted for 10% of the metal 3D printing market in 2020 [5]. The fundamental characteristic of ME printing technology is the extrusion of material layer by layer through a print head to form 3D components. Unlike metal powder-based printing processes, ME printing technology involves extruding materials in the form of filaments. These filaments are flexible materials made from a mixture of metal powder and binding

agents [6, 7]. ME printing technology is used to print the components as shown in Figure 1. The ME printing machine consists of two spools, one containing the printing material and the other containing ceramic material used to print the separators between the product and the build plate or between the product and support structures. During printing, the print head heats the printing material above the melting temperature of the polymer binder, extruding the softened material onto the build plate. The print head moves up and down along the vertical z-axis, extruding each layer of material evenly. Simultaneously, the build plate moves in the x-y direction, shaping the form of the component. The ceramic material is printed as a barrier between the component and support structures or as a separation layer between the component and the build plate to facilitate easy removal of the product after the sintering process. The printing nozzle extrudes filaments with circular cross-sections, layer by layer. There are gaps between the layers, which reduce adhesion between the metal layers and can cause deformation during the sintering process in Figure 2.

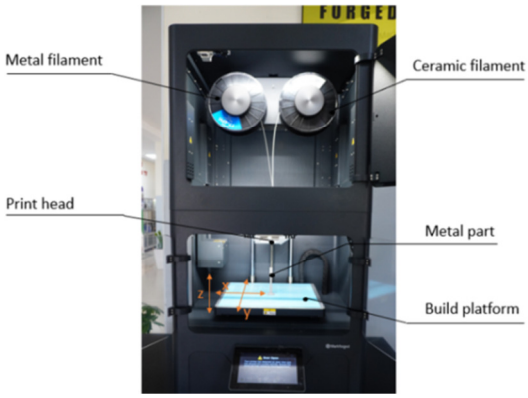

Fig. 1. The Markforged Metal X 3D printer used for experimental printing.

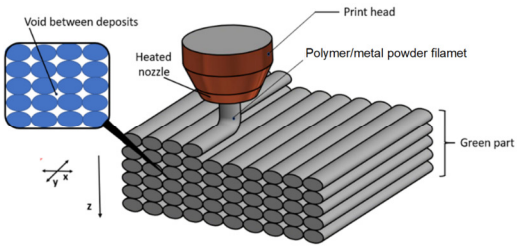

Fig. 2. Printing process and the gaps between the printed layers.

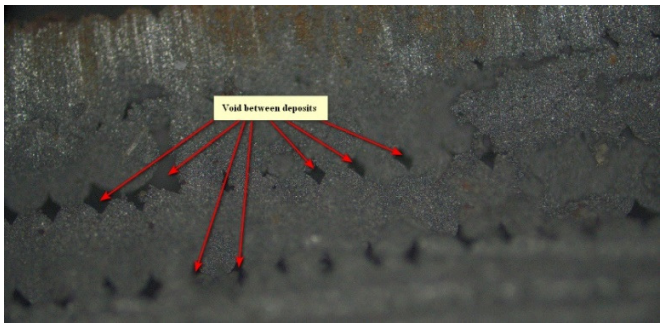

Fig. 3. The voids between deposits of the product before sintering

The as-printed or "green" part undergoes a debinding process known as "washing." The delicate and loosely bound workpiece is placed inside a heated debinding machine, where a solvent is used to dissolve a portion of the core component of the binder system. The binder system plays a significant role in influencing the production process and the quality of the final component. Typically, it consists of three main components: polymers, waxes, and additives. It can be further classified into the core, the backbone, and the additive. The core component constitutes 50-90% of the volume and includes materials with low viscosity that are easily dissolved and can undergo catalytic degradation. These materials are effectively removed during the initial debinding stage. The backbone component accounts for 0-50% of the volume and consists of materials that are resistant to debinding solvents. This component helps maintain the strength of the debound part before sintering, such as polyolefins. The final additive can make up 0-10% of the volume of the binder system. The core component is gradually dissolved, leaving behind the backbone, which is referred to as being in its "brown" state. The brown part retains much of the backbone but remains highly porous. Subsequently, the part is placed into a furnace and subjected to a gradual increase in temperature from ambient to 70-90% of the metal's melting point. This thermal process decomposes the residual support component of the binder system. As the temperature rises within the furnace, solid bonds or necks start to form between the metal powder particles, thereby reducing the surface energy of the part. Upon reaching the metal's melting point, atomic diffusion of the metal particles occurs, leading to the formation of solid bonds. This reduces porosity and transforms the loosely bound metal powder into a theoretically dense metal part with a density of 96-99.8%. This densification process results in shrinkage of the part by 12-20%, which is taken into account by the system's software during the file transfer stage [8].

The surface quality of metal 3D printing is assessed through various parameters, including hardness, residual stress on the surface layer, and surface roughness. Among these parameters, surface roughness plays a significant role in the performance and lifespan of the machine component and is often chosen as a key evaluation criterion in production processes. Surface roughness is evaluated based on the profile of the surface texture formed between the intersection of the actual surface of the component and a plane perpendicular to the actual surface. Two parameters, average roughness (R_a) and peak-to-valley height (R_z), are used to draw conclusions [9, 10]. Specialized surface roughness measuring devices are used to determine the surface roughness of the component. It is typically measured in micrometers (µm) or microinches (µin). High surface roughness can result in increased friction, reduced component durability, and decreased dimensional accuracy. The effects of printing parameters on surface roughness in the Metal Additive Manufacturing (MAM) have been studied by various authors. For example, authors in [11] considered the effect of printing orientation on the surface roughness and microstructure in selective laser melting of Ti-6Al-4V. This study investigates the effect of print orientation on surface roughness and microstructure in the selective laser melting of Ti-6Al-4V. The authors found that print orientation has a significant impact on

surface roughness, with parts printed vertically exhibiting higher roughness than those printed horizontally. The microstructure of the printed parts was also found to be orientation-dependent. This study provides important insights for optimizing the selective laser melting process for Ti-6Al-4V. Authors in [12] investigated the influence of building orientation on surface roughness in the selective laser melting of Inconel 718. They found that print orientation has a significant impact on surface roughness, with parts printed vertically exhibiting higher roughness than those printed horizontally. The authors suggest that this is due to differences in cooling rates and thermal gradients during the printing process. This study provides important insights for optimizing the selective laser melting process for Inconel 718. Authors in [13] found that print orientation has a significant impact on surface quality and mechanical properties, with parts printed horizontally exhibiting better surface quality and higher mechanical properties than those printed vertically. This study provides important insights for optimizing the electron beam melting process for Ti-6Al-4V. Authors in [14] investigated the relationship between the surface roughness and the mechanical properties in the selective laser melting of stainless steel. They found that print orientation has a significant impact on both surface roughness and mechanical properties, with parts printed vertically exhibiting higher roughness and lower mechanical properties than those printed horizontally. This study provides important insight for optimizing the selective laser melting process for stainless steel.

The aim of the present paper is to introduce a novel geometrical model for the prediction of surface roughness in lateral walls within the context of ME printing. This model takes into consideration the diverse print orientations, and its simulated results are systematically compared with the experimental data. Tensile specimens were meticulously printed in three different orientations: Flat, on-edge, and upright. Surface roughness was evaluated along the generatrix of the samples, employing a contact roughness meter for precise measurements. Subsequently, the model results are rigorously compared to the experimental data, encompassing different print orientation angles, to assess the accuracy and reliability of the predictive model. The scientific novelty of the current study lies in the development of a comprehensive geometrical model, specifically designed for surface roughness prediction in lateral walls during the ME printing process. The integration of various print orientations and its comparison with the experimental results enhance the understanding of surface roughness variations in the 3D printing of metal components. This research holds practical relevance as it aims to optimize printing parameters, thereby improving the overall quality and performance of metal parts produced through ME technology. By providing valuable insight into surface roughness prediction, this study contributes to advancements in metal additive manufacturing processes, towards more efficient and reliable manufacturing practices.

II. SURFACE ROUGHNESS MODEL

Due to the circular structure of the printing nozzle, the surface of the product in ME printing technology tends to have a large surface roughness, because the metal powder mixture, after being extruded, tends to deform in an elliptical shape due to the gravitational force between the layers. In theory, the surface roughness of metal printing using ME technology can be preliminarily calculated from the printing parameters. Figure 4 illustrates a typical surface structure after printing.

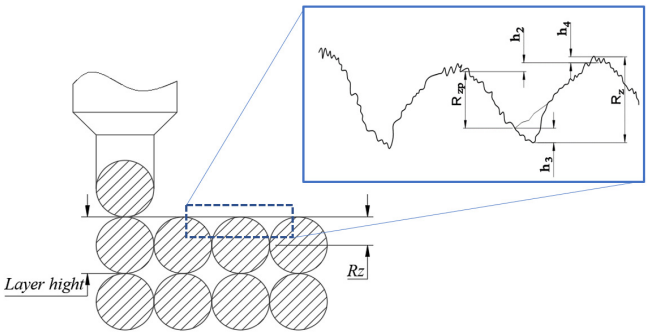

Fig. 4. Formation diagram of the surface roughness during the printing process.

The height of surface roughness R_z can be calculated using the formula:

$$R_z = R_{zp} + \Delta R_z$$

$$\Delta R_z = h_2 + h_3 + h_4$$

where R_z is the average height of the total absolute values of the 5 highest peaks and the 5 deepest valleys of the profile within the standard evaluation length (L), ΔRz is the amount by which the actual height of the surface roughness exceeds the theoretically calculated value, h_2, h_3, and h_4 represent the components of surface roughness corresponding to the influence of printer nozzle size, size variations during the washing process, and size variations of the printing material during the sintering process, respectively, and R_{zp} is the calculated theoretical height of surface roughness.

III. COMPARISON BETWEEN THE PREDICTED VALUES AND THE EXPERIMENTAL RESULTS

The experimental results using 17-4 PH stainless steel as the printing material on the Markforged Metal X 3D printer in the additive manufacturing laboratory at Vinh Long University of Technology Education, Vinh Long City, Vietnam, as shown in Figure 1, will be compared with the calculated values. The printed samples are tensile test specimens, which were printed in three orientations: flat, on-edge, and upright (Figure 5). For each orientation, 5 samples were printed and the surface roughness was measured at 3 different positions. The printing paths on the outermost layer corresponding to each type are illustrated in Figure 6. The post-sintered layer height was set to 0.127 mm.

Figure 7 showcases the results of the produced samples after undergoing the printing, washing, and sintering stages. It is worth mentioning that the samples printed in the upright position and subsequently sintered have a tendency to fracture into multiple pieces. This can be attributed to the layering arrangement and the influence of gravity during the solidification process, which heightens the risk of deformation and eventual fracturing of the part.

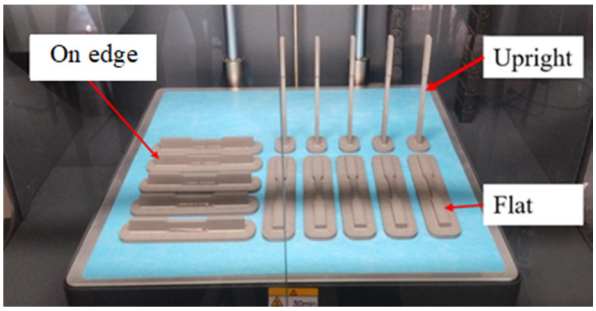

Fig. 5. The experimental test samples.

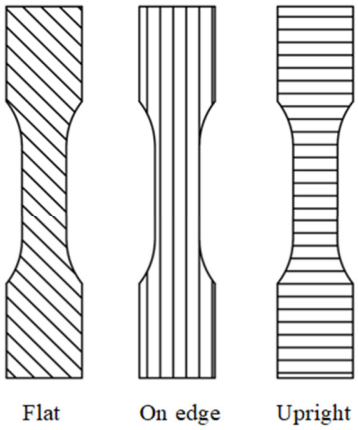

Fig. 6. The structure of the outermost printing path for each orientation.

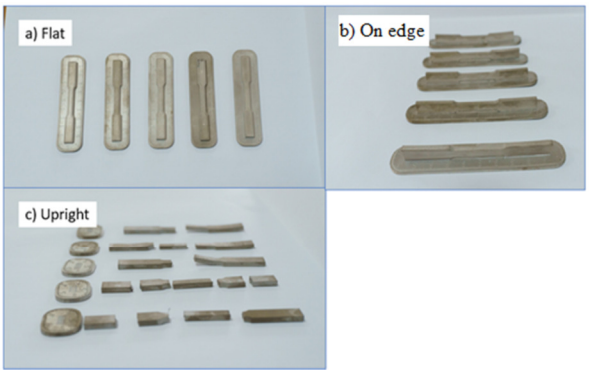

Fig. 7. Sample components after the printing process.

The parameters regarding the layer height and printing direction used in the experimental process are shown in Table I. The surface layer structure of the printed samples and the probe's scanning direction of the measuring instrument are presented in Figure 9. Each sample was measured at 3 different positions: at the clamp end, in the transition area, and in the middle of the sample. The average value of each measurement was then calculated. Five samples were measured for each printing direction, and the average value was obtained. The average surface roughness values of the 5 experimental samples when printing 17-4 PH stainless steel in 3 different directions are presented in Table I.

From the measurement results, it can be observed that there are differences in surface roughness among the different printing orientations. The smoothest surface is achieved in the Upright orientation, with average R_a and R_z values of 7.42 µm and 40.49 µm, respectively. This is because the peaks and valleys of the surface roughness are relatively uniform (Figure 8) and of negligible magnitude. The comparison chart of predicted and calculated surface roughness values can be seen in Figure 10, constructed based on the data in Table I.

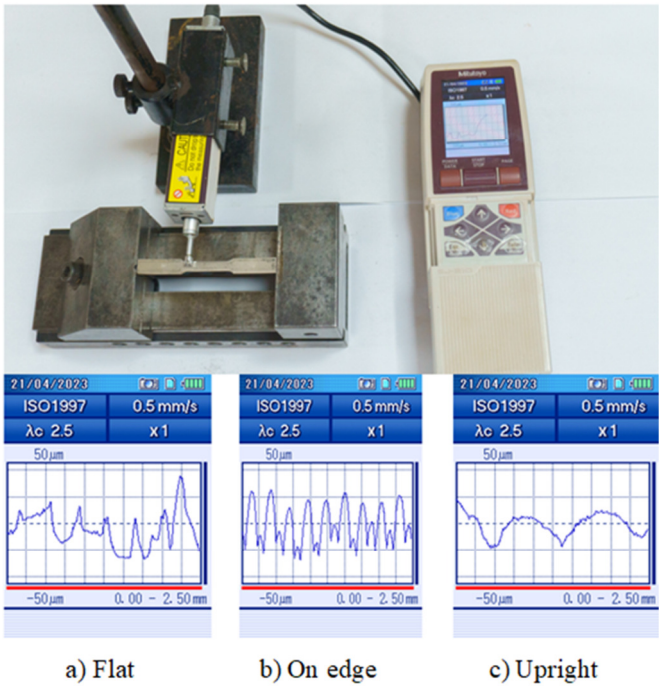

Fig. 8. Measuring with the Mitutoyo SJ-210 surface roughness device.

TABLE I. AVERAGE SURFACE ROUGHNESS

Printing material: 17-4 PH stainless steel Post-sintered layer height (mm): 0.127				
Printing orientation	**Surface roughness, Rz (µm)**			
	Experimental surface roughness values		**Calculated**	**Deviation calculated**
	$R_{z(Exp)}$	$R_{a(Exp)}$	$R_{zp(calcul)}$	
Flat	82.83	16.92	60	27.5%
On-edge	69.42	16.05	63.5	8.5%
Upright	40.49	7.42	40	1.2%

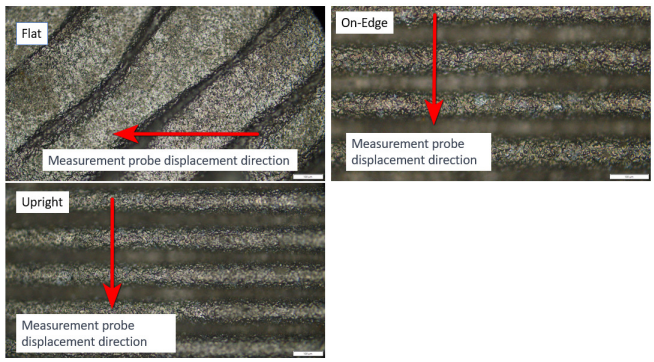

Fig. 9. Surface structure of the sample detail and probe movement direction of the surface roughness measurement device.

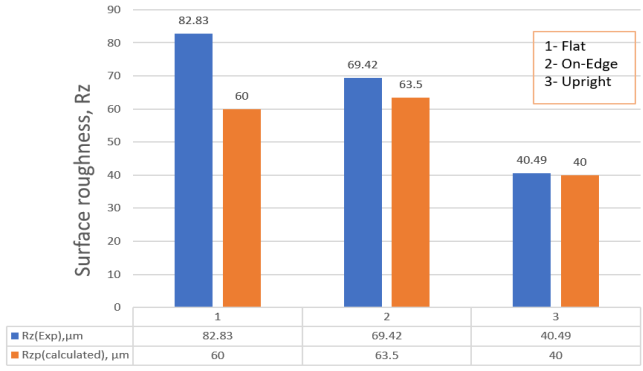

Fig. 10. Surface roughness in different printing orientations: experimental and predicted values.

It can be seen in Table I and Figure 10 that the best surface roughness is achieved in the upright orientation, with an average experimental roughness value of 40.49 µm and a theoretical calculated roughness value of 40 µm, resulting in a 1.2% average deviation. In the On-edge orientation, the experimental surface roughness value is 69.42 µm, while the theoretical value is 63.5 µm, resulting in an average deviation of approximately 8.5% between the theoretical and experimental results. In the flat orientation, which exhibits the highest surface roughness, the average roughness value of the experimental samples is 82.83 µm, while the theoretical value is 60 µm, resulting in a deviation of 27.5%. These findings indicate that the printing orientation significantly influences the surface roughness, and the surface roughness prediction method presented in this study can be effectively used to predict the surface roughness in specific cases.

IV. CONCLUSION

Based on the experimental results and the following analysis, we can draw the following conclusions: Surface roughness in metal 3D printing is evaluated using parameters such as R_a and R_z. The printing orientation significantly affects the surface roughness. In the case of using 17-4 PH stainless steel as the printing material, the upright orientation achieves the best surface smoothness, while the flat orientation has the highest roughness. There are discrepancies between the experimental and the calculated surface roughness values. However, the surface roughness prediction method presented in this study can be used to estimate surface roughness in specific cases.

This research provides valuable information about surface roughness in metal 3D printing and the influence of printing orientation. It can support the design and optimization of the manufacturing process using metal 3D printing technology.

ACKNOWLEDGMENT

The work described in this paper was supported by the Vinh Long University of Technology Education for a scientific project.

REFERENCES

[1] R. Citarella and V. Giannella, "Additive Manufacturing in Industry," *Applied Sciences*, vol. 11, no. 2, Jan. 2021, Art. no. 840, https://doi.org/10.3390/app11020840.

[2] D. G. Zisopol, D. V. Iacob, and A. I. Portoaca, "A Theoretical-Experimental Study of the Influence of FDM Parameters on PLA Spur Gear Stiffness," *Engineering, Technology & Applied Science Research*, vol. 12, no. 5, pp. 9329–9335, Oct. 2022, https://doi.org/10.48084/etasr.5183.

[3] D. G. Zisopol, I. Nae, A. I. Portoaca, and I. Ramadan, "A Statistical Approach of the Flexural Strength of PLA and ABS 3D Printed Parts," *Engineering, Technology & Applied Science Research*, vol. 12, no. 2, pp. 8248–8252, Apr. 2022, https://doi.org/10.48084/etasr.4739.

[4] D. G. Zisopol, M. Minescu, and D. V. Iacob, "A Theoretical-Experimental Study on the Influence of FDM Parameters on the Dimensions of Cylindrical Spur Gears Made of PLA," *Engineering, Technology & Applied Science Research*, vol. 13, no. 2, pp. 10471–10477, Apr. 2023, https://doi.org/10.48084/etasr.5733.

[5] L. Cherdo, "Metal 3D printers in 2023: a comprehensive guide," *Aniwaa*, Jun. 2022. https://www.aniwaa.com/buyers-guide/3d-printers/best-metal-3d-printer/.

[6] J. Gonzalez-Gutierrez, S. Cano, S. Schuschnigg, C. Kukla, J. Sapkota, and C. Holzer, "Additive Manufacturing of Metallic and Ceramic Components by the Material Extrusion of Highly-Filled Polymers: A Review and Future Perspectives," *Materials*, vol. 11, no. 5, May 2018, Art. no. 840, https://doi.org/10.3390/ma11050840.

[7] N. H. Hiep, L. H. Ky, P. H. Anh, L. H. K. Duyen, and T. V. Hung, "An Evaluation of Some Specifications of Turbine Blades Made by 3D Printing Technology and Processed on CNC Milling Machines," in *Advances in Engineering Research and Application*, 2023, pp. 177–187, https://doi.org/10.1007/978-3-031-22200-9_19.

[8] M. Armstrong, H. Mehrabi, and N. Naveed, "An overview of modern metal additive manufacturing technology," *Journal of Manufacturing Processes*, vol. 84, pp. 1001–1029, Dec. 2022, https://doi.org/10.1016/j.jmapro.2022.10.060.

[9] N. V. Cuong and N. L. Khanh, "Improving the Accuracy of Surface Roughness Modeling when Milling 3x13 Steel," *Engineering, Technology & Applied Science Research*, vol. 12, no. 4, pp. 8878–8883, Aug. 2022, https://doi.org/10.48084/etasr.5042.

[10] H. K. Le, "Multi-Criteria Decision Making in the Milling Process Using the PARIS Method," *Engineering, Technology & Applied Science Research*, vol. 12, no. 5, pp. 9208–9216, Oct. 2022, https://doi.org/10.48084/etasr.5187.

[11] P. Hartunian and M. Eshraghi, "Effect of Build Orientation on the Microstructure and Mechanical Properties of Selective Laser-Melted Ti-6Al-4V Alloy," *Journal of Manufacturing and Materials Processing*, vol. 2, no. 4, Dec. 2018, Art. no. 69, https://doi.org/10.3390/jmmp2040069.

[12] D. Du *et al.*, "Influence of build orientation on microstructure, mechanical and corrosion behavior of Inconel 718 processed by selective laser melting," *Materials Science and Engineering: A*, vol. 760, pp. 469–480, Jul. 2019, https://doi.org/10.1016/j.msea.2019.05.013.

[13] J. Bruno, A. Rochman, and G. Cassar, "Effect of Build Orientation of Electron Beam Melting on Microstructure and Mechanical Properties of Ti-6Al-4V," *Journal of Materials Engineering and Performance*, vol. 26, no. 2, pp. 692–703, Feb. 2017, https://doi.org/10.1007/s11665-017-2502-4.

[14] H. H. Alsalla, C. Smith, and L. Hao, "Effect of build orientation on the surface quality, microstructure and mechanical properties of selective laser melting 316L stainless steel," *Rapid Prototyping Journal*, vol. 24, no. 1, pp. 9–17, Jan. 2018, https://doi.org/10.1108/RPJ-04-2016-0068.